

Preparation of MoVTe(Sb)Nb mixed oxide catalysts using a slurry method for selective oxidative dehydrogenation of ethane

Qi Xie, Luqian Chen*, Weizheng Weng, Huilin Wan*

State Key Laboratory for Physical Chemistry of the Solid Surfaces, Department of Chemistry and Institute of Physical Chemistry, Xiamen University, Xiamen 361005, PR China

Received 29 June 2005; received in revised form 30 June 2005; accepted 2 July 2005
Available online 8 August 2005

Abstract

The preparation of bulk MoVTe(Sb)Nb mixed oxide catalysts using a traditional slurry method, results in highly active catalysts for oxidative dehydrogenation of ethane to ethene. Several major phases including orthorhombic M1, hexagonal M2 or $\text{Mo}_x\text{M}_{1-x}\text{O}_{2.8}$ ($M = \text{V}$ or Nb) have been detected in the catalysts from characterization results such as X-ray diffraction (XRD), SEM and EDX analyses. Ethane conversion and yield to ethene increase with increasing content of the M1 phase in the catalysts. The maximum yield of ethene (ca. 87% selectivity and ca. 90% conversion, $\text{STY}_{\text{C}_2\text{H}_4}$ of $176 \text{ g kg}_{\text{cat}}^{-1} \text{ h}^{-1}$) has been obtained with a $\text{MoV}_{0.31}\text{Te}_{0.2}\text{Nb}_{0.14}$ mixed oxide catalyst, calcined at 873 K under nitrogen, containing almost pure orthorhombic M1 phase and small amounts of unidentified impurity phases, operating at a relatively low reaction temperature of 673 K. The orthorhombic M1 phase has been shown to be the most active in ethane activation and the most selective for ethene formation. The hexagonal M2 phase is relatively inactive in ethane activation and less selective for ethene formation. The Te-free phases such as $\text{Sb}_4\text{Mo}_{10}\text{O}_{31}$ and $\text{Mo}_x\text{M}_{1-x}\text{O}_{2.8}$ ($M = \text{V}$ or Nb) show the lowest selectivity to ethene.

© 2005 Elsevier B.V. All rights reserved.

Keywords: Ethene; MoVTe(Sb)Nb mixed oxide catalyst; Selective oxidation of ethane; Slurry method; ODHE

1. Introduction

The current abundance and low cost of short chain alkanes makes them ideal feedstocks for the oxidative dehydrogenation (ODH) of alkanes as an attractive alternative route to light olefins. In particular, the ODH of ethane to ethene (ODHE), which is usually obtained by a highly endothermic thermal pyrolysis. It is known that the catalytic dehydrogenation of ethane to ethene is prone to coking which results in a short catalyst life-time [1]. In contrast, ODHE could overcome the thermodynamic limitation in the direct dehydrogenation reaction by coupling the dehydrogenation and hydrogen oxidation steps. The presence of oxygen limits coking and extends the catalyst life-time. A few stud-

ies on ODHE over different kinds of catalysts have been reported in both patents and academic literature [1–11]. These studies have mainly involved non-reducible catalysts (i.e. Li/MgO based [1–4], fluoride-containing rare/alkaline earth-based [5,6] and LiCl/sulfated ZrO_2 [7]) with reaction temperatures of more than 873 K and reducible metal oxide catalysts (e.g. Mo and/or V-based [1,2], MoV-based [8] and MoVNb-based [9–12]) with reaction temperatures of less than 823 K. Wang et al. [7] have reported a non-reducible Nd-doped LiCl/sulfated ZrO_2 catalyst which gives 97% conversion of ethane and 84% selectivity to ethene at a reaction temperature of 923 K. However, a short catalyst lifetime was observed. In contrast, Mo–V–Nb based reducible mixed oxide systems seem more promising catalysts with lower reaction temperatures and higher yields of ethane. In particular, 73% conversion of ethane and 71% selectivity to ethene has been obtained over a $\text{Mo}_{0.61}\text{V}_{0.26}\text{Nb}_{0.07}\text{Sb}_{0.04}\text{Ca}_{0.02}\text{O}_x$

* Corresponding authors.

E-mail address: lq_chen@yahoo.com (L. Chen).

catalyst at a reaction temperature of 673 K [10]. Recently, Nieto et al. [11,12] reported the hydrothermal synthesis of MoVTeNb mixed oxide catalysts for ODHE and the catalytic activity is strongly influenced by the heat-treatment temperature. They obtained an 88.5% conversion of ethane and 81% selectivity to ethene at a reaction temperature of 673 K over the MoVTeNb mixed oxide catalyst heat-treated at 923 K. The catalytic performance in ethane oxidation could be related to the presence of the orthorhombic $\text{Te}_2\text{M}_{20}\text{O}_{57}$ (M = Mo, V or Nb) phase in cooperation with the Mo_5O_{14} -type phase.

In this study, the catalytic performances of MoV-based mixed oxide catalysts, modified with Te(Sb) and Nb for ODHE, prepared using a traditional slurry method [13–17], are reported. Circa 90% conversion of ethane and ca. 87% selectivity to ethene have been obtained at a reaction temperature of 673 K over a MoVTeNb mixed oxide catalyst, calcined at 873 K under nitrogen, containing the orthorhombic M1 phase and small amounts of impurity phases. The active phase and catalytic centers for ODHE have also been discussed.

2. Experimental

2.1. Catalyst preparation

A series of bulk $\text{Mo}_1\text{V}_{0.3}\text{Te}(\text{Sb})_{0.2}\text{Nb}_{0.1}$, $\text{Mo}_1\text{V}_{0.32}\text{Te}_{0.5}\text{Nb}_{0.1}$, $\text{Mo}_1\text{V}_{0.32}\text{Te}_{0.33}\text{Nb}_{0.1}$ and $\text{Mo}_1\text{V}_{0.31}\text{Te}_{0.2}\text{Nb}_{0.14}$ mixed oxide catalysts with various concentrations of the orthorhombic M1 phase [18–20] were prepared respectively by the traditional slurry method, as follows:

Ammonium metavanadate was dissolved in 70 ml distilled water at 353 K to give a yellow solution. Telluric acid and ammonium heptamolybdate were added to form an orange solution to the desired molar ratio (or antimony trioxide and ammonium heptamolybdate were added at 353 K with stirring for 12 h to get a blue solution). The solutions were cooled to room temperature (RT) and an aqueous solution of niobium oxalate was then added to each one with stirring for 30 min. The suspensions were evaporated by a rotary evaporator under vacuum (less than 0.08 MPa) at 323 K and dried at 393 K. The solids obtained were calcined at 793 and 873 K, respectively for 2 h under flowing nitrogen.

MoO_x , $\text{Mo}_1\text{V}_{0.3}$ and $\text{Mo}_1\text{V}_{0.3}\text{Nb}_{0.1}$ mixed oxide catalysts were also prepared as a comparison based on the above preparation procedure.

Catalytic testing was performed in a tubular fixed bed flow quartz reactor (i.d. 5 mm) under atmospheric pressure at a reaction temperature of 673 (or 713)K using 500 mg of catalyst, GHSV = 600 h^{-1} . The feed composition was C_2H_6 , O_2 and N_2 in the molar ratio 1/1/1.3. The mixed feed and the reaction products were analyzed on-line by gas chromatography equipped with TCD detection. A Porapak Q column was used to separate CO_2 , C_2H_6 and C_2H_4 , etc. A 5 Å molecular sieve column was used to separate O_2 , N_2 , CH_4 ,

CO, etc. Conversion, selectivity and yield were defined as follows:

conversion of ethane

$$= (\text{moles } \text{C}_2\text{H}_6 \text{ consumed} / \text{moles } \text{C}_2\text{H}_6 \text{ charged}) \times 100,$$

selectivity to product

$$= (\text{moles product} / \text{moles } \text{C}_2\text{H}_6 \text{ consumed}) \\ \times (\text{mole number of carbon atoms in a mole product} / 2) \\ \times 100,$$

yield to product

$$= (\text{selectivity to product} \times \text{conversion of ethane}) / 100$$

The main reaction products e.g. ethene, CO and CO_2 were detected. Carbon balances were always more than 99% under the reaction conditions. Appropriate blank test experiments using an empty reactor and an empty reactor filled with quartz wool were carried out at 733 K under the studied atmosphere. No ethane conversion was observed, demonstrating that the contribution of a homogeneous reaction could be neglected under the studied reaction conditions.

2.2. Catalyst characterization

X-ray diffraction (XRD) patterns were recorded on a Rigaku Rotflex D/Max-C diffractometer using Cu $\text{K}\alpha$ radiation ($\lambda = 0.15418 \text{ nm}$) at 40 kV \times 30 mA in Bragg's angles (2θ) 5–60°.

Nitrogen adsorption and desorption isotherms (BET) were recorded on an automate Micromeritics Tri-Star3000 apparatus at 77 K.

The chemical compositions were determined by EDX carried out on a TECNAI F30 high-resolution transmission electron microscope (point resolution 0.2 nm) equipped with an EDAX analyzer. SEM images were captured using a FESEM LEO-1530 scanning electron microscope operated at 10 kV.

Photoelectron spectra (XPS) were recorded on a Quantum 2000 Scanning ESCA Microprobe electron spectrometer using Al $\text{K}\alpha$ radiation with a pass energy of 46.95 eV. The binding energy (BE) scale was regulated by setting the C 1s transition at 284.6 eV. The accuracy of the BE was $\pm 0.1 \text{ eV}$.

3. Results and discussion

BET surface areas of samples b–e are shown in Table 1. Low surface areas (4–10 m^2/g) are observed in all cases. The results of quantitative EDX and XPS analyses given in Table 1 indicate that bulk chemical compositions of the calcined samples are close to their corresponding theoretical compositions. In contrast, higher molar ratios V/Mo and Nb/Mo are observed for surface chemical compositions of

Table 1
Characteristics of samples a–e calcined at 793 K under nitrogen

Sample	Specification	S_{BET} (m ² /g)	Mo/V/Te/Nb molar ratio	
			EDX composition	XPS composition
a	MoO _x	–	–	–
b	Mo ₁ V _{0.3} O _x	4	1/0.23–0.6/0/0	1/0.4/0/0
c	Mo ₁ V _{0.3} Nb _{0.1} O _x	10.3	1/0.24/0/0.09	1/0.37/0/0.18
d	Mo ₁ V _{0.3} Sb _{0.2} Nb _{0.1} O _x	8.1	1/0.2/0.15/0.1	1/0.26/0.21/0.11
e	Mo ₁ V _{0.3} Te _{0.2} Nb _{0.1} O _x	4.3	1/0.28/0.19/0.12	1/0.2/0.17/0.09

S_{BET} : BET surface area; EDX composition: the chemical composition determined by EDX analysis; XPS composition: the chemical composition determined by XPS analysis.

the MoV and MoVNb mixed oxide catalysts, relative to their theoretical compositions.

XRD patterns at $2\theta = 5\text{--}60^\circ$ of samples a–e calcined at 793 K under nitrogen show that no phase changes occur in the samples d and e (MoVTe(Sb)Nb mixed oxides) before or after testing (patterns before testing are not shown), indicating that the structures of the samples d and e are very stable during the studied reaction conditions. However, some changes of phases occur in the samples a–c (MoO_x, MoV and MoVNb mixed oxides) after testing. Fig. 1 shows XRD patterns at $2\theta = 5\text{--}60^\circ$ of the samples a–e after testing. After testing the MoO₃ phase is dominant in MoO_x. Mo sub-oxides such as Mo₈O₂₃ (or Mo₉O₂₆), MoO₃ and (V_xMo_{1-x})₅O₁₄ as major phases are observed in sample b without Te or Nb. (M_xMo_{1-x})₅O₁₄ (M = V or Nb) as a major phase and small amounts of MoO₃ phase are present in the sample c without Te. Moreover, Sb₄Mo₁₀O₃₁ and (M_xMo_{1-x})₅O₁₄ (M = V or Nb) as major phases and small amounts of MoO₃ are present in the sample d (MoVSbNb mixed oxides). The XRD pattern obtained for samples e (MoVTeNb mixed oxides) show diffraction peaks at 2θ (°) = 7.9, 9.0, 13.0, 13.9, 14.6, 22.1, 23.4, 24.9, 26.2, 26.6, 26.9, 27.2, 28.2, 29.2, 30.5, 31.4, 35.3, 36.2, 45.2, 50.0 and 54.2 associated with the presence of small amounts of Mo_xM_{1-x}O_{2.8} (M = V or Nb) and new complex crystalline phases namely M1 and M2, which correspond to orthorhombic Te₂M₂₀O₅₇ (M = Mo, V or Nb) and hexagonal Te_{0.33}MO_{3.33} (M = Mo, V or Nb) (2θ (°) = 22.1, 28.2, 36.2, 45.2 and 50.0), respectively [21–27]. However, there are differences in the details of the compositional and structural makeup of the phases, reported by Grasselli et al. [18–20].

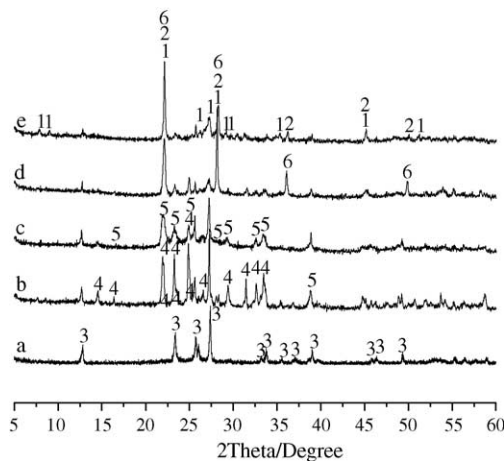


Fig. 1. XRD patterns of samples a–e calcined at 793 K in nitrogen after testing. 1: Te₂M₂₀O₅₇ (M = Mo, V or Nb) (M1 phase [18–27]); 2: Te_{0.33}MO_{3.33} (M = Mo, V or Nb) (M2 phase [18–27]); 3: MoO₃ (JCPDS #35–0609); 4: Mo sub-oxide such as Mo₈O₂₃ (JCPDS #05–0339) or Mo₉O₂₆ (JCPDS #05–0441 or 12–0753); 5: (M_xMo_{1-x})₅O₁₄ (M = V or Nb) (JCPDS #31–1437 or 27–1310); 6: Sb₄Mo₁₀O₃₁ (JCPDS #33–0104).

According to the report, the compositions of the hexagonal phase and the orthorhombic phase are Mo₆Te₂VO₂₀ and Mo_{7.5}V_{1.5}NbTeO₂₉, respectively.

The reaction results of samples a–e calcined at 793 K in nitrogen and sample f–i calcined at 873 K in nitrogen are summarized in Table 2 and Fig. 4, respectively. Ethene, CO and CO₂ are the main reaction products. Oxygenated products other than CO_x have not been observed during the

Table 2
Testing results of samples a–e

Sample	Phases detected by XRD	$S_{\text{C=}}$ (%)	S_{CO_2} (%)	S_{CO} (%)	Conv. (%)	STY _{C₂H₄} (g kg _{cat} ⁻¹ h ⁻¹)
Reactor + quartz wool	/	/	/	/	/	/
a	MoO ₃	52.1	47.9	0.0	0.13	0.15
b	Mo ₈ O ₂₃ , Mo ₉ O ₂₆ , MoO ₃ and (V _x Mo _{1-x}) ₅ O ₁₄	57.9	31.6	10.5	9.4	12.4
c	(M _x Mo _{1-x}) ₅ O ₁₄ (M = V or Nb) (S) and MoO ₃ (W)	58.0	28.2	13.8	36.1	47.6
d	Sb ₄ Mo ₁₀ O ₃₁ (S), (M _x Mo _{1-x}) ₅ O ₁₄ (M = V or Nb) (S) and MoO ₃ (W)	61.9	26.6	11.5	45.6	64.2
e	M1 (S), M2 (W) and (M _x Mo _{1-x}) ₅ O ₁₄ (M = V or Nb) (W)	91.9	6.4	1.7	65.0	135.8

Catalyst weight 500 mg; reaction at 713 K and atmospheric pressure using a feed of composition C₂H₆/O₂/N₂(1/1/1.3); GHSV 600 h⁻¹. S: selectivity; conv.: conversion; C=: C₂H₄; (W): weak; (S): strong.

reaction. It has been shown that MoO_x is inactive for ODHE (0.13% conversion and 52% selectivity). Ethane conversion and selectivity to ethene increase a little by adding V into MoO_x (Table 2, row 3). A further increase in conversion and surface area (shown in Table 1) are observed by adding Nb into MoV mixed oxides, while selectivity to ethene does not change (Table 2, row 4). The XRD patterns b and c in Fig. 1 show that $(\text{M}_x\text{Mo}_{1-x})_5\text{O}_{14}$ ($\text{M} = \text{V}$ or Nb) is present as the major phase in the MoV and MoVNb mixed oxides, respectively. It is therefore proposed that the $(\text{M}_x\text{Mo}_{1-x})_5\text{O}_{14}$ ($\text{M} = \text{V}$ or Nb) phase is effective on ethane activation during the catalytic reaction and also on the deep oxidation of ethane to CO_x . The ethane conversion increases further, when Sb is added into the MoVNb mixed oxides. At the same time, the selectivity to ethene increases a little (Table 2, row 5). The XRD pattern for sample d in Fig. 1 shows that MoVSbNb mixed oxide catalyst contains several main phases, such as $(\text{M}_x\text{Mo}_{1-x})_5\text{O}_{14}$ ($\text{M} = \text{V}$ or Nb) and $\text{Sb}_4\text{Mo}_{10}\text{O}_{31}$, the structures of which are known to be isomorphous to that of the hexagonal $\text{Te}_{0.33}\text{MO}_{3.33}$ ($\text{M} = \text{Mo}, \text{V}$ or Nb) phase [22,27]. This indicates that the $\text{Sb}_4\text{Mo}_{10}\text{O}_{31}$ phase in cooperation with an amount of $(\text{M}_x\text{Mo}_{1-x})_5\text{O}_{14}$ ($\text{M} = \text{V}$ or Nb) phase appears to be more effective on activation of ethane and selective formation of ethene during ODHE than the $(\text{M}_x\text{Mo}_{1-x})_5\text{O}_{14}$ ($\text{M} = \text{V}$ or Nb) phase. It's noteworthy that the conversion and selectivity to ethene significantly increase (Table 2, row 6) when Te is added into the MoVNb mixed oxides instead of Sb. Moreover, no change in yield of ethene after 72 h of reaction (catalyst life-time) is observed, indicating that the MoVTeNb mixed oxide catalysts are very stable during the reaction. XRD pattern for sample e shows that the sample contains several phases such as orthorhombic M1 and small amounts of hexagonal M2 and $\text{Mo}_x\text{M}_{1-x}\text{O}_{2.8}$ ($\text{M} = \text{V}$ or Nb). This indicates that the presence of the orthorhombic M1 phase in the sample results in higher conversion of ethane and selectivity in ethene.

XRD analyses of the samples f–i (Fig. 2) show that the hexagonal M2 phase and small amounts of

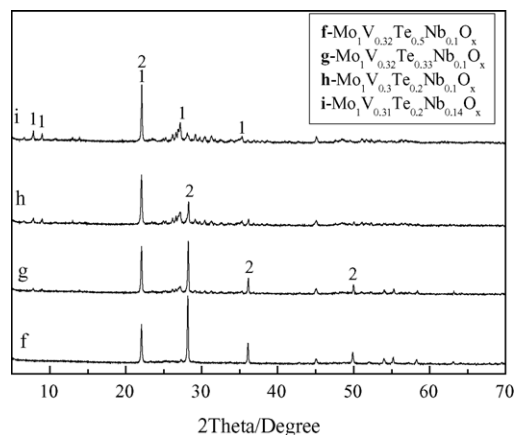


Fig. 2. XRD patterns of samples f–i calcined at 873 K in nitrogen after testing. 1: $\text{Te}_2\text{M}_{20}\text{O}_{57}$ ($\text{M} = \text{Mo}, \text{V}$ or Nb) (M1 phase); 2: $\text{Te}_{0.33}\text{MO}_{3.33}$ ($\text{M} = \text{Mo}, \text{V}$ or Nb) (M2 phase).

unidentified impurity phases are present in the sample f ($\text{Mo}_1\text{V}_{0.32}\text{Te}_{0.5}\text{Nb}_{0.1}\text{O}_x$). The orthorhombic M1 phase and small amounts of unidentified impurity phases are present in the sample i ($\text{Mo}_1\text{V}_{0.31}\text{Te}_{0.2}\text{Nb}_{0.14}\text{O}_x$). The orthorhombic M1 phase, the hexagonal M2 phase and small amounts of other minor phases are present in samples g ($\text{Mo}_1\text{V}_{0.32}\text{Te}_{0.33}\text{Nb}_{0.1}\text{O}_x$) and h ($\text{Mo}_1\text{V}_{0.3}\text{Te}_{0.2}\text{Nb}_{0.1}\text{O}_x$), respectively. M1/(M2 + M1) molar ratios in the samples g and h are estimated to be ca. 30 and 75%, respectively [18]. SEM images (Fig. 3) of the samples show that the morphology

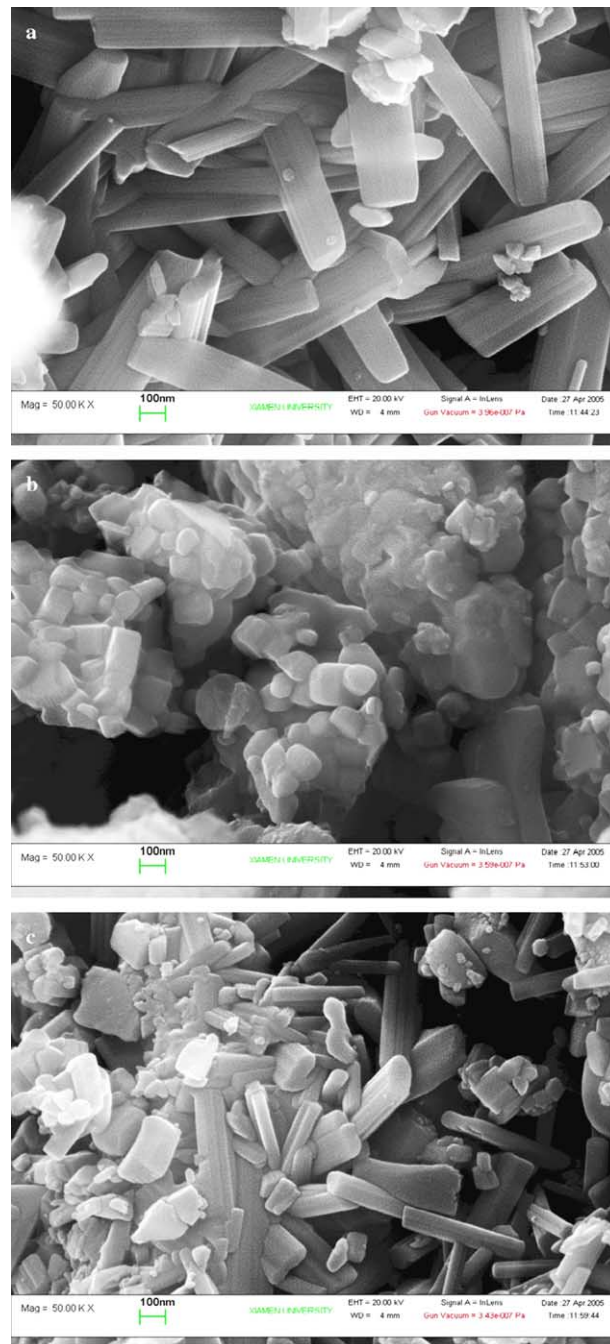


Fig. 3. (a) SEM image of sample i (M1 phase); (b) SEM image of sample f (M2 phase); (c) SEM image of sample h (a mixture of M1 and M2 phases).

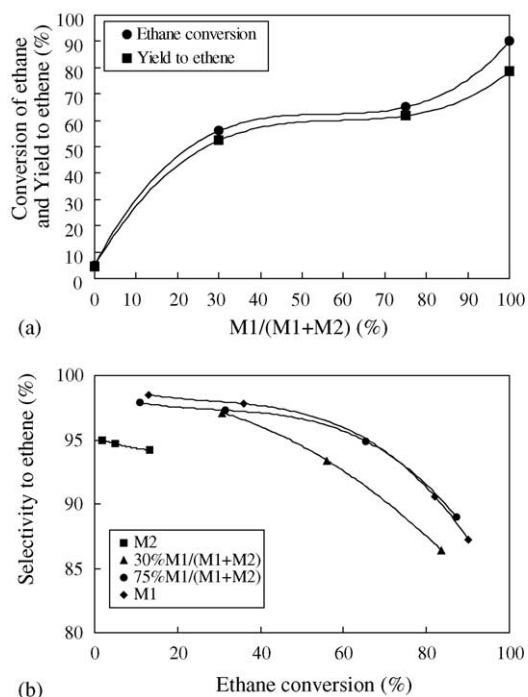


Fig. 4. Catalytic performances of samples f–i calcined at 873 K under nitrogen for ODHE. Catalyst weight 500 mg; $C_2H_6/O_2/N_2(1/1/1.3)$; GHSV 600 h^{-1} ; reaction temperature at 673 K (a) conversion of C_2H_6 and yield to C_2H_4 vs. content of M1 phase in the samples and (b) selectivity to C_2H_4 vs. conversion of C_2H_6 over the samples with various contents of M1 phase.

of the M1 phase is needle-like, while the M2 phase crystallizes in platelets. A mixture of the needle-like M1 phase and platelet-like M2 phase is observed in the sample h. The observations are consistent with earlier reports [18,28]. Local EDX analyses for the needle-like and platelet-like crystals show that the compositions of the crystals are homogeneous and respectively close to average compositions $Te_2M_{20}O_{57}$ and $Te_{0.33}MO_{3.33}$ ($M = Mo, V$ or Nb) reported by Millet et al. [22,27].

Catalytic performances of samples f–i with various M1 contents for ODHE are shown in Fig. 4. Fig. 4(a) shows that a good catalytic performance of MoVTeNbO catalysts for ODHE can mainly be related to the presence of the M1 phase. Conversion of ethane and yield to ethene increase with increasing the content of the M1 phase in the sample. Very low conversion of ethane is obtained over the sample f containing almost pure M2 phase. The maximum conversion of ethane and yield to ethene are obtained over the sample i containing almost pure M1 phase. Fig. 4(b) shows that very high selectivities to ethene are obtained over the samples h and i, especially for the sample i containing almost pure M1 phase. The hexagonal M2 phase presents relatively lower selectivity in formation of ethene. Therefore, it can be reasonably concluded that the orthorhombic M1 phase is the most active phase for ethane activation and the most selective phase for ethene formation.

It is well known that MoVTeNbO catalysts are effective and will most likely be used in industry for producing acrylic

acid and acrylonitrile by selective oxidation and ammoxidation of propane [13–22,27,28]. Catalytic centers of the catalysts in the ammoxidation are multimetallic and multifunctional. The orthorhombic M1 phase is catalytically the most effective for the conversion of propane to acrylonitrile (or acrylic acid) [13–22,27,28], where a V^{5+} surface site ($V^{5+} = O \leftrightarrow 4^+V^{\bullet}-O^{\bullet}$) is associated with paraffin activation by abstracting a methylene-H from propane, a Te^{4+} site with the methyl-H abstraction (from paraffin) or α -H abstraction once the olefin has formed, and a $(Mo^{6+})_2$ site with the NH insertion. Four Nb^{5+} centers, each surrounded by five molybdenum octahedral, stabilize and structurally isolate the catalytically active centers from each other [18]. The hexagonal M2 phase is ineffective for paraffin activation because it does not contain any V^{5+} centers. However, it is known to be effective for the conversion of olefins [18–22,27,28]. The behavior for ODHE is different to that described above on the same catalysts. A V^{5+} surface site ($V^{5+} = O \leftrightarrow 4^+V^{\bullet}-O^{\bullet}$) in the orthorhombic M1 phase is thus proposed to be associated with ethane activation by abstracting a methyl-H from ethane. Because ethene is known to be more stable than ethane, the good catalytic performance observed on the catalysts is due to both the high activity in the oxidative activation of ethane and relative inactivity in ethene oxidation.

4. Conclusions

MoVTeNbO_x catalysts, prepared by the traditional slurry method, calcined at a temperature of 873 K under nitrogen, present highly selective and active for ODHE due to the presence of the orthorhombic M1 phase. The $Te_2M_{20}O_{57}$ ($M = Mo, V$ or Nb) phase represents the most selective phase for ethene formation and the most active phase for ethane activation. The $Sb_4Mo_{10}O_{31}$, $Te_{0.33}MO_{3.33}$ ($M = Mo, V$ or Nb) and $Mo_xM_{1-x}O_{2.8}$ ($M = V$ or Nb) phases are relatively inactive in the ethane activation. The good catalytic performance observed on the catalysts is due to both the high activity in the oxidative activation of ethane and relative inactivity in ethene oxidation. An effective crystalline MoVTeNbO_x catalyst, for the production of ethene using a low-cost feedstock e.g. ethane, should contain the exclusively enriched orthorhombic M1 phase, in particular pure orthorhombic M1 phase, to ensure an extremely high ethane conversion and ethene selectivity.

Acknowledgements

The financial support of SRF for ROCS, SEM, the National Priority Fundamental Research Project of China (No. G1999022408) and the National “973” Project of China (No. 2005CB221408) is gratefully acknowledged. We also greatly thank Dr. Christopher J.A. Bingham and Dr. J.S. Hargreaves for their very valuable suggestions.

References

- [1] F. Cavani, F. Trifiró, *Catal. Today* 24 (1995) 307.
- [2] M. Bañaes, *Catal. Today* 51 (1999) 319.
- [3] E. Morales, J.H. Lunsford, *J. Catal.* 118 (1989) 255.
- [4] S. Fuchs, L. Leveles, K. Seshan, L. Lefferts, A. Lemonidou, J. Lercher, *Top. Catal.* 15 (2001) 169.
- [5] C. Au, X. Zhou, *J. Chem. Soc. Faraday Trans.* 93 (1997) 485.
- [6] H. Wan, X. Zhou, W. Weng, R. Long, Z. Chao, W. Zhang, M. Chen, J. Luo, S. Zhou, *Catal. Today* 51 (1999) 161.
- [7] S. Wang, K. Murata, T. Hayakawa, S. Hamakawa, K. Suzuki, *Chem. Commun.* (1999) 103;
S. Wang, K. Murata, T. Hayakawa, S. Hamakawa, K. Suzuki, *Catal. Lett.* 59 (1999) 173 and 191.
- [8] W. Ueda, N.F. Chen, K. Oshihara, *Chem. Commun.* (1999) 517.
- [9] E.M. Thorsteinson, T.P. Wilson, F.G. Young, P.H. Kasai, *J. Catal.* 52 (1978) 116.
- [10] J.H. McCain, US Patent 4,524,236 (1985).
- [11] J.M. López Nieto, P. Botella, M.I. Vázquez, A. Dejoz, *Chem. Commun.* (2002) 1906;
J.M. López Nieto, P. Botella, M.I. Vázquez, A. Dejoz, WO Patent 03/064035 (2003).
- [12] P. Botella, E. García-González, A. Dejoz, J.M. López Nieto, M.I. Vázquez, J. González-Calbet, *J. Catal.* 225 (2004) 428.
- [13] M. Hatano, A. Kayo, European Patent 318,295 (1988).
- [14] S. To, M. Takahashi, S. Hirose, Toa Gosei Chem. Ltd., JP 10,137,585 (1996).
- [15] M.M. Lin, *Appl. Catal. A: Gen.* 207 (2001) 1;
M.M. Lin, *Appl. Catal. A: Gen.* 250 (2003) 287.
- [16] R.K. Grasselli, *Catal. Today* 49 (1999) 141.
- [17] L. Chen, E.G. Derouane, J.C. Védrine, *Appl. Catal. A: Gen.* 270 (2004) 157.
- [18] R.K. Grasselli, J.D. Burrington, D.J. Buttrey, P. DeSanto Jr., C.G. Lugmair, A.F. Volpe, T. Weingand, *Top. Catal.* 23 (2003) 5.
- [19] P. DeSanto Jr., D.J. Buttrey, R.K. Grasselli, C.G. Lugmair, A.F. Volpe, B.H. Toby, T. Vogt, *Top. Catal.* 23 (2003) 23.
- [20] J. Holmberg, R.K. Grasselli, A. Andersson, *Top. Catal.* 23 (2003) 55.
- [21] T. Ushikubo, K. Oshima, A. Kayou, M. Hatano, *Stud. Surf. Sci. Catal.* (1997) 473.
- [22] M. Aouine, J.L. Dubois, J.M.M. Millet, *Chem. Commun.* (2001) 1180.
- [23] Magneli, *Acta Chem. Scand.* 7 (1953) 315.
- [24] L. Kihlberg, *Acta Chem. Scand.* 13 (1959) 954;
L. Kihlberg, *Acta Chem. Scand.* 14 (1960) 1612.
- [25] T. Ekström, M. Nygren, *Acta Chem. Scand.* 26 (1972) 1828.
- [26] T. Ekström, M. Nygren, *Acta Chem. Scand.* 26 (1972) 1836.
- [27] J.M.M. Millet, M. Baca, A. Pigamo, D. Vitry, W. Ueda, J.L. Dubois, *Appl. Catal. A: Gen.* 244 (2003) 359.
- [28] K. Oshihara, T. Hisano, W. Ueda, *Top. Catal.* 15 (2001) 153.